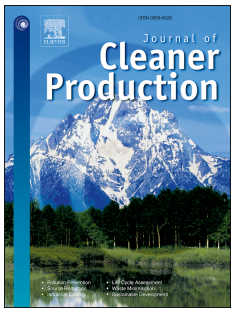

Effects of lockdown due to COVID-19 outbreak on air quality and anthropogenic heat in an Industrial belt of India

Swades Pal, Priyanka Das, Indrajit Mandal, Rajesh Sarda, Susanta Mahato, Kim-Anh Nguyen, Yuei-An Liou, Swapan Talukdar, Sandipta Debanshi, Tamal Kanti Saha

PII: S0959-6526(21)00894-5

DOI: https://doi.org/10.1016/j.jclepro.2021.126674

Reference: JCLP 126674

To appear in: *Journal of Cleaner Production*

Received Date: 16 July 2020

Revised Date: 5 March 2021

Accepted Date: 6 March 2021

Please cite this article as: Pal S, Das P, Mandal I, Sarda R, Mahato S, Nguyen K-A, Liou Y-A, Talukdar S, Debanshi S, Saha TK, Effects of lockdown due to COVID-19 outbreak on air quality and anthropogenic heat in an Industrial belt of India, *Journal of Cleaner Production*, https://doi.org/10.1016/j.jclepro.2021.126674.

Effects of lockdown due to COVID 19 outbreak on air quality and anthropogenic heat in an Industrial belt of India

Credit author statement

Swades Pal: Conceptualization, Methodology, Writing- Original draft preparation, Investigation, Writing- Original draft preparation, Writing- Reviewing and Editing., Supervision.

Priyanka Das: Writing- Reviewing and Editing

Indrajit Mandal: Methodology, Software, Formal analysis, Visualization, Data curation

Rajesh Sarda: Methodology, Software, Formal analysis, Visualization, Data curation

Susanta Mahato: Methodology, Software, Formal analysis, Visualization, Data curation, Writing- Original draft preparation, Writing- Reviewing and Editing.,

Kim-Anh Nguyen: Writing- Original draft preparation, Writing- Reviewing and Editing

Yuei-An Liou: Investigation, Methodology, Writing- Original draft preparation, Writing- Reviewing and Editing, Supervision, Project administration, Funding acquisition.

Swapan Talukdar: Writing- Original draft preparation

Sandipta Debanshi: Writing- Original draft preparation, Writing- Reviewing and Editing

Tamal Kanti Saha : Writing- Original draft preparation

Effects of lockdown due to COVID-19 outbreak on air quality and anthropogenic heat in an Industrial belt of India

Swades Pal
Assistant Professor, Department of Geography,University of Gour Banga,Malda,India
Email : swadespal2017@gmail.com

Priyanka Das
Assistant Professor, Department of Geography,Malda Women's College,Malda,India
Email : priyankadas694@gmail.com

Indrajit Mandal
Research Scholar,Department of Geography,University of Gour Banga,Malda,India
Email: indrajitgeofarakka@gmail.com

Rajesh Sarda
Research Scholar,Department of Geography,University of Gour Banga,Malda,India
Email: rajeshsarda127@gmail.com

Susanta Mahato
Senior Research Fellow, Department of Geography,University of Gour Banga,Malda,India
Email: mahatosusanta2011@gmail.com

Kim-Anh Nguyen
Postdoc Fellow, Center for Space and Remote Sensing Research (CSRSR), National Central University, Taoyuan 32001, Taiwan.
Email: nguyenrose@csrsr.ncu.edu.tw

Yuei-An Liou
Distinguished Professor, Center for Space and Remote Sensing Research (CSRSR), National Central University, Taoyuan 32001, Taiwan.
Email: yueian@csrsr.ncu.edu.tw

Swapan Talukdar
Senior Research Fellow, Department of Geography,University of Gour Banga,Malda,India
Email: swapantalukdar65@gmail.com

Sandipta Debanshi
Research Scholar,Department of Geography,University of Gour Banga,Malda,India
Email : debanshi.sandipta93@gmail.com

Tamal Kanti Saha
Senior Research Fellow, Department of Geography,University of Gour Banga,Malda,India
Email : tamalkantisaha999@gmail.com

Acknowledgments:

This research was financially supported by the Ministry of Science and Technology (MOST) of Taiwan under the codes MOST 109-2923-E-008-004-MY2 and MOST 108-2111-M-008-036-MY2.

Graphical Abstract

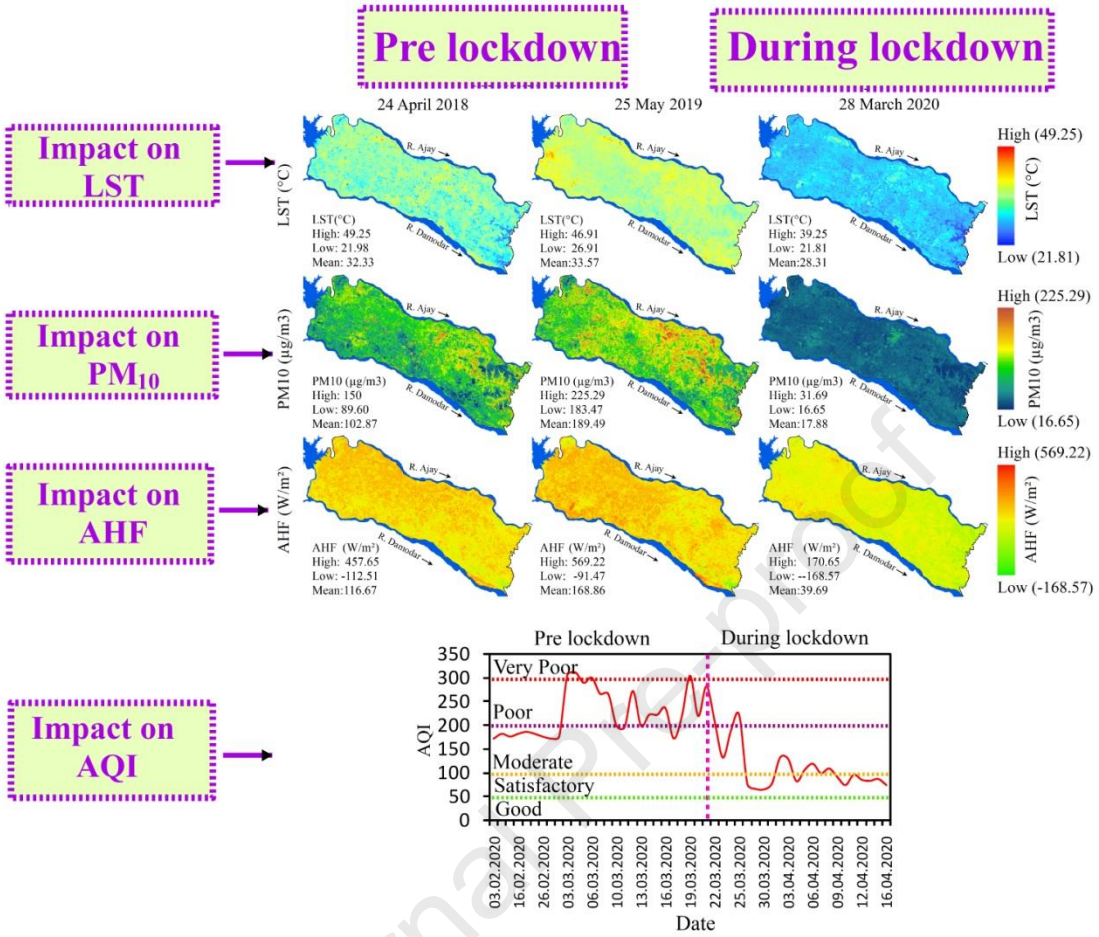

Effects of lockdown due to COVID-19 outbreak on air quality and anthropogenic heat in an industrial belt of India

Abstract

Highly urbanized and industrialized Asansol Durgapur industrial belt of Eastern India is characterized by severe heat island effect and high pollution level leading to human discomfort and even health problems. However, COVID-19 persuaded lockdown emergency in India led to shut-down of the industries, traffic system, and day-to-day normal work and expectedly caused changes in air quality and weather. The present work intended to examine the impact of lockdown on air quality, land surface temperature (LST), and anthropogenic heat flux (AHF) of Asansol Durgapur industrial belt. Satellite images and daily data of the Central Pollution Control Board (CPCB) were used for analyzing the spatial scale and numerical change of air quality from pre to amid lockdown conditions in the study region. Results exhibited that, in consequence of lockdown, LST reduced by 4.02ºC, PM_{10} level decreased from 102 to 18µg/m^3 and AHF declined from 116 to 40W/m^2 during lockdown period. Qualitative upgradation of air quality index (AQI) from *poor to very poor state* to *moderate to satisfactory state* was observed during lockdown period. To regulate air quality and climate change, many steps were taken at global and regional scales, but no fruitful outcome was received yet. Such lockdown (temporarily) is against economic growth, but it showed some healing effect of air quality standard.

Keywords: Lockdown; Industrial belt; Land surface temperature; Anthropogenic heat flux and Air quality index

1. Introduction

Climate change is among the highly argued topics in the contemporary world. The accelerated rise of global temperature and consequence has been among the vital concerns since 1850 (IPCC, 2013). Growing energy footprint was condemned as the dominant cause behind the rise of temperature (Aydin and Turan 2020). There is worldwide variation in energy footprint, usually high in the developed countries and low in the underdeveloped or developing countries. In the USA per capita, the carbon emission rate is 14.9 metric tons,

while, in India, it is only 1.57 metric tons. Massive combustion of fossil fuel in industrial, urban, and transport sectors, and consequent emission of carbon lead to temperature rise and air quality degradation (Zhang et al., 2020). The increased concentration of particulate matter, SO_2, CO, etc causes deterioration of air quality (Xieand Deng., 2020; Dutta and Gupta 2021). Recently anthropogenic heat flux (AHF) in the highly urbanized and industrial sectors is another emerging concern (Nguyen et al., 2018; Liou et al., 2019; Yu et al., 2021). Anthropogenic heat means heat release to the atmosphere resulted from human activities like combustion of fossil fuel, human metabolism, industrial emission, thermally sensitive building materials, and traffic emission (Zheng et al., 2021). Ayanlade and Howard (2019) focused on the estimation of AHF from satellite images for the last two decades. Varquez et al. (2021) estimated future urban expansion and climate change effect in futuristic AHF. In this context, most of those works tried to compute AHF from image data. It was reported that estimated anthropogenic heat from the image was greater than source-specific field data-centric estimated heat (Wang et al., 2020), but field data based in situ measurements are highly dependent on data availability (Firozjaei et al., 2020) and in the third world country which puts a hindrance on such studies. On the other hand, remote sensing-based image data has become an alternative which helps to retrieve AHF of larger geographical area (Raj et al., 2020). From the previous studies, it became clear that with increasing human pressure and anthropogenic activities, AHF is getting enhanced and the global eco-environment has become more vulnerable (Nguyen and Liou, 2019a, b). Jin et al. (2020) reported the successful use of Landsat and MODIS data for estimating LST and anthropogenic heat distribution over Delhi and its surrounding region during both winter and summer seasons. It was observed that during 2000-2010 AHF (W/m^2) had increased by nearly 150% over the settlement and solid structures.

In India, several studies carried out by a good number of researchers like Mandal et al. (2020); Plocoste et al. (2021) investigated time series LST trend and PM level. Mahato and Pal (2018) focused on impact of land surface parameters on land surface temperature regime. Most of the studies reported the increasing trend of LST and PM in the urban and industrial area across the world. Moreover, spatial image data released from European Space Agency (EPA), NASA also reported a growing PM level in the atmosphere in most urban halves of the world. Growing economic activities like intensification in industry, transport, tourism, agriculture, and trade are the majorly responsible for this (Mandal et al., 2020). Nevertheless, fast-changing land use/land cover, squeezing green and blue space over the terrestrial land,

qualitative deterioration of terrestrial and aquatic ecosystems, and weakening of self-regulatory mechanism of the ecosystem are unable to refresh and restore the environment due to release of high-volume pollutants within a very short period (Du et al., 2020). A good number of world summits like annual United Nations Climate Change Conference (UNCOP) from 1995 till present were conducted; Intergovernmental Panel on Climate Change (IPCC) was periodically conducted with climate change contents reported, but no-good solution was found yet to combat the environmental deterioration. To keep the continuous economic growth, no strict measure was yet taken compromising with production volume.

However, COVID-19 pandemic started to outbreak since the second fortnight of December 2019 around the world. Since beginning this disease rapidly spread over China, Italy, France, Spain, Germany, Russian federation, UK, USA, India, UAE, Australia Brazil, Argentina and many other countries. Till 25th of October it snatched more than 1,147,000 people and infected more than 42,500,000 people. Considering this emergency and to stop the threat of this virus, most of the world implemented lockdown (full or partial) since March 2020, which simultaneously froze the pollution effective economic sectors like industry, transport, tourism, etc. (Muhammad et al., 2020). This imposed measure caused a great economic loss around the world, but the nature got the opportunity to refresh its environment as demonstrated by Tobias et al. (2020). These studies clearly articulated the healing of air quality. A sharp and sudden fall of global carbon emission was observed due to the reduction in energy footprint (Wang and Su, 2020), stoppage of production in industry (Muhammad et al., 2020), break-in public traffic (Chen et al., 2020) etc. Temporary halt of economic activities not only reduced the carbon emission, but also restricted the discharge of several other Greenhouse Gases (GHGs) and pollutants like Sulfur Dioxide (SO_2), Nitrogen Dioxide (NO_2), and Particulate Matters 2.5 and 10 ($PM_{2.5,\ 10}$) (NASA, 2020). In addition, about 25% reduction in CO_2, equivalent to 1million tons of carbon, was detected in China (Wang and Su, 2020). Mahato et al. (2020) carried out work on mega city Delhi, India and reported significant quality improvement in most parts of Delhi. Mahato and Ghosh (2020) reported most polluted Indian cities air quality conditions during the lockdown amid COVID-19. Sharma et al. (2020) reported AQI across 22 cities of India depicting improvement by 15-44%. Das et al. (2021) experienced that the air quality of the Indian megacities also improved by 50% amid lockdown and air quality hotspot has diluted amid lockdown but restored in partial lockdown. Travaglio et al. (2021) reported the crucial role of level of NOx and particulate matter to trigger COVID-19 infection in the UK. Zhang et al. (2021) have

statistically shown the association between COVID-19 spread and air pollution in China. Ju et al. (2021) experienced that in Korea air pollution level has been identically reduced during the pandemic of COVID-19. From heavy industry dominated areas of North and Northeast China, the emission of NO_2 extensively reduced in the first week of lockdown (European Space Agency, 2020). Almost 50% crash in air pollution in New York City (USA) was identified in March 2020 in comparison to the same period of 2019 (Saadat et al., 2020). NO_2 emission cut rate was also significantly high in different European countries, like Spain, UK, Italy, France, Germany as captured by satellite images (Ficetola and Rubolini, 2020). $PM_{2.5}$, PM_{10}, CO_2, and NO_2 concentration levels reduced by 43%, 31%, 10%, and 18%, respectively, in comparison to previous year over 22 Indian cities (Sharma et al., 2020). Apart from air quality improvement, Bashir et al. (2020) also found a strong positive association of air quality indicators with other climatic variables. It is the fact that increment of greenhouse gases can enhance the temperature retaining capacity of the atmosphere and this, in turn, regulates several other components of climate (Xu and Cui, 2021). The Smog Effect in megacities like Delhi is very well known to the world among this.

The existing works conducted regarding the environmental perspective of the COVID-19 outbreak were focused either on entire world or on mega-cities, while what is the response of industrial area dominated cities beyond megacities was not addressed so far. In India, Sathe et al. (2021), Naqvi et al. (2021), Das et al. (2021), Mele and Magazzino (2021) and Mor et al. (2021) figured out the impact on air quality over city scale. In this regard, a lack of study was noticed addressing the improvement of air quality due to COVID-19 persuaded lockdown in heavy manufacturing based fast growing urban-industrial area influenced both by the primary and secondary economic activities of a third world nation. Beside air quality, rise of temperature caused by anthropogenic activities was another global concern that should be examined under the offsetting effects of lockdown, which did not receive enough attention. However, urban dominated industrial sector is a major source of greenhouse gases and anthropogenic heat. These research gaps can be addressed in reference to a world reputed large scale industrial area called Asansol Durgapur development region of Eastern India. This highly urbanized and densely populated region is characterized by simultaneous insertion of a primary economic sector like coal mining and a secondary economic sector in form of large industries along with two municipal corporations and three municipalities. The area is well known for heat island effect and high pollution level due to the coupled effects of urban expansion and industrial pollution. A fast-growing urban area with high population density

demands huge energy in mining, industrial, traffic and domestic sectors and emits diverse pollutants notably greenhouse gases. In India such proximate and dense association of urban sites, mining and industrial activities within an area is very rare in India. Study over this region in this aspect is not available. High temperature (40ºC or more during summer season (April-May)), intensive urban growth, mining and industrial activities and high energy footprint are responsible for creating high intensity heat island effects, ejection of huge pollutants, which in turn caused for degrading air quality in this area. In addition, a huge amount of black particles that are ejected from the mining sites, which not only increase the concentration of particulate matters in the air, but also enhance the heat absorbing capacity intensifying heat island effect of the region. All these characteristics have inspired to select this urban-industry dominated area as a case. Lockdown situation has brought an opportunity to justify how far anthropogenic activities are responsible for creating heat island effect, AHF and air pollution, since the major economic sectors were stopped working. The gap of thermal state, AHF and pollution level between pre and amid lockdown may crudely highlight the role of anthropogenic activities in this regard. AHF is often neglected but its role is important for studying thermal effect. In this view, the present study intended to examine whether lockdown causes temporary dilution of heat island, reducing the AHF and improving the air quality and how far anthropogenic activities are responsible for heat island effect, growing AHF and pollution level.

2. Materials and methods

This industrial region (Fig. 1) is a planning area with coverage more than 1,600 km^2 administered by the Asansol-Durgapur Development Authority (ADDA) and represents one of the eight major industrial regions of India. Steel plants of the Steel Authority of India Limited (SAIL) and Indian Iron and Steel Company (IISCO) are the prime industries in this region. These industries are supported by coal, iron, and steel. Besides the Steel and Coal based industries, the region also consists of some other heavy industries, such as Durgapur Chemicals, Durgapur Thermal Power Station, Dishergarh Power Supply, Damodar Valley Power Corporation, etc. Eventually air pollution level is usually found high in this region in a normal situation. Apart from these, the region is characterized by the sub-humid monsoon climate with high seasonal difference in temperature between winter (December to January) and summer season (March to May). In addition, intensive economic activities make this region a densely populated urban where more than three fourth (77%) of its total population (2,400,000 people) is concentrated in the urban areas far above Indian average.

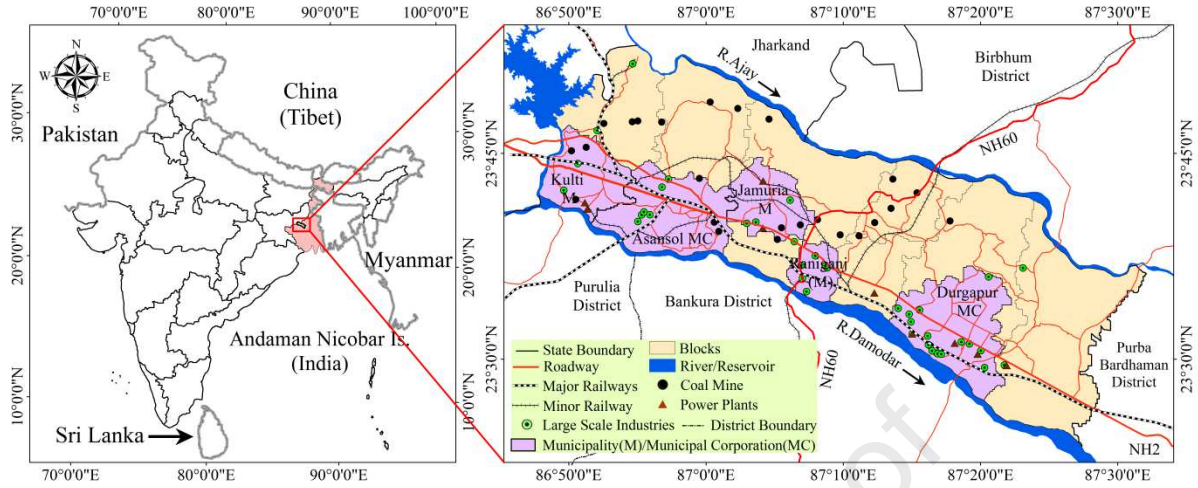

Fig. 1: Geo-location of the study area along with different administrative units and other supplementary information like the location of coal mines, large scale industries, and minor roads.

For estimating surface temperature, PM_{10} and anthropogenic heat flux, and Landsat images were involved. USGS website was subscribed to download images (path/row: 139/44, spatial resolution: 30m) dated on 24th April 2018 and 25th May 2019 for the pre-lockdown periods and on 28th March 2020 for the amid lockdown period. Daily average data of seven air pollutants, namely particulate matter of two separate diameters ($PM_{2.5}$ and PM_{10}), Nitrogen Dioxide (NO_2), Sulphur Dioxide (SO_2), Ozone (O_3), Carbon Monoxide (CO), and Ammonia (NH_3), were extracted from the online portal containing air quality data of Central Pollution Control Board (CPCB).

Land surface temperature (LST), particulate matter 10 (PM_{10}) and anthropogenic heat flux (AHF) were computed at pixel scale from Landsat images for both pre and during lockdown periods. For showing the pre-lockdown state, images of 24th April 2018 and 25th May 2019 and during the lockdown state of 28th March 2020 were taken. Apart from this, daily data on PM_{10}, $PM_{2.5}$, SO_2, CO, NO_2, NH_3 and O_3 both for pre and during lockdown were taken into consideration for showing the effect.

2.1 Computation of Land surface temperature (LST) and validation

All the objects having a temperature above zero (K) radiate thermal electromagnetic energy. Analyzing the radiation balance at the land-air interface, it is possible to extract LST with the

help of satellite images. The three most commonly used methods for LST computation are (1) Radiative Transfer Equation (2) Single-Channel Algorithm (3) Split-Window Algorithm. Among these methods, Garcia-Santos et al. (2018) reported a computable radiative transfer equation better than the others. Considering this, the present work applied this method for computing LST from image data (Eq. 1).

LST computation follows multi-step like (1) Conversion of the Digital Number (DN) to Spectral Radiance, (2) conversion of spectral radiance to at satellite brightness temperature, (3) LST extraction, (4) conversion of LST from Kelvin to degree Celsius. This method is quite different in different sensors (Landsat 5, 7, 8). The detail method is available in the guidelines put forward by the Landsat Project Science Office (2002). Detail steps for computing LST are also given in supplementary material 1.

$$\text{LST} = \frac{T_B}{[1+\{(\lambda \times TB/\rho) \times In\varepsilon\}]} \quad \text{(Eq. 1)}$$

where λ is the wavelength of radiated radiance in meter (Markham and Barker, 1985), ε is land surface emissivity, $\rho = h * c/\sigma$ ($1.438*10^{-2} m\text{-}K$), h is Planck constant ($6.626*10^{-34}$ J-s), σ is Boltzmann constant ($1.38*10^{-23}$ *J/K*), and c is the velocity of light ($2.998*10^{8}$ m/s). Note that LST estimated by Eq. (1) is in Kelvin.

Satellite data derived LST maps were validated with field measurements collected at 37 sites across the study area in pre-lockdown period using thermal infrared thermometer. During lockdown, LST map was validated using only three sites due to access restriction. Pearson's correlation coefficient (r) was then computed to assess the spatial association.

2.2 Estimating particulate matter 10 (PM_{10}) concentration

Landsat 8 Operational Land Imager (OLI) data of USGS was taken for estimating PM_{10}. Retrieval of PM_{10} from Landsat image was done by many scholars like Saraswat et al. (2017) following the basic guideline of USGS: Landsat 8 Handbook, 2016. It follows following steps like (1) Translation of DN value to Top of Atmospheric (TOA) radiance, (2) Translation of DN value to TOA reflectance, (3) Sun angle corrected TOA reflectance, (4) Atmospheric correction, (5) Path Radiance correction, (6) Aerosol optical thickness (AOT) estimation, (7) AOT and PM_{10} correlation, and (8) Derivation of particulate matter (PM_{10}).

After computing and mapping PM_{10}, validation of the map was done using Tem-top airing-1000 air quality monitor (measuring range 0-999 µg/m^3, resolution 0.1 µg/m^3) derived field data at 80 sites for pre-lockdown period. However, it was not possible to validate maps of

lockdown phase using all those sites due to assess limitations. Field measurements from only three sites including the monitoring station of CPCB were taken for validating the map. Pearson's correlation coefficient was computed between the data derived from PM_{10} image and field data.

2.3 Estimating anthropogenic heat flux (AHF)

The anthropogenic heat consists of the total heat discharged from industries, vehicles, and human activities. In urban and industrially rich areas, AHF is a significant heat contributor. For computing spatial AHF, spatial data layers like net radiation, ground heat flux, latent heat, sensible heat, are necessary. Net radiation (R_n) denotes actual availability of solar radiant energy at surface. It is the major component of surface energy balance and gets influenced by surface albedo. In case of industry dominated urban area anthropogenic heat (A) was incorporated in the equation of surface energy balance which is a sum of total heat released from industry, transportation and human activities. The rate of energy which is transmitted by soil per unit time and area is referred as ground heat flux (G). The loss of heat due to gradients of temperature is referred as sensible heat flux whereas latent heat flux (L) an additional parameter of surface energy balance. First, all these data layers were computed and based on equations 2 and 1. Figure 2 represents the spatial state of these parameters. Finally, we estimated AHF following Zhang et al. (2013). The modified energy balance equation ($R_n+A=G+H+L$) Following Oke 1987 is the basis of computing AHF. This energy balance equation was modified and differently developed for the heavy industrial and densely populated urban areas where surface energy balance is different from natural landscape because of the addition of huge amount of anthropogenic heat to the flux component. Present study area belongs to this category for having both heavy industry and dense population. Apart from that several other recent studies like Kotthaus and Grimmond, (2014); Ward et al., (2016); Ziaul and Pal, (2018) successfully used this method to quantify AHF of urban settlements. The particular method is provided in supplementary 1.

Anthropogenic heat discharge, expressed as $H_n$is estimated through the expression given below in Eq. (2):

$$H_n = R_n - G - LE \qquad \text{(Eq. 2)}$$

The difference between total sensible heat flux (H) and H_n is known as anthropogenic heat flux (H_{as}) and was estimated by the equation:

$$H_{as} = H - H_n \quad \text{(Eq. 3)}$$

It was only calculated if H was higher than or equivalent to H_n. We can use Eq. (3) to calculate H_{as}. If not, it was a substitute for H_n.

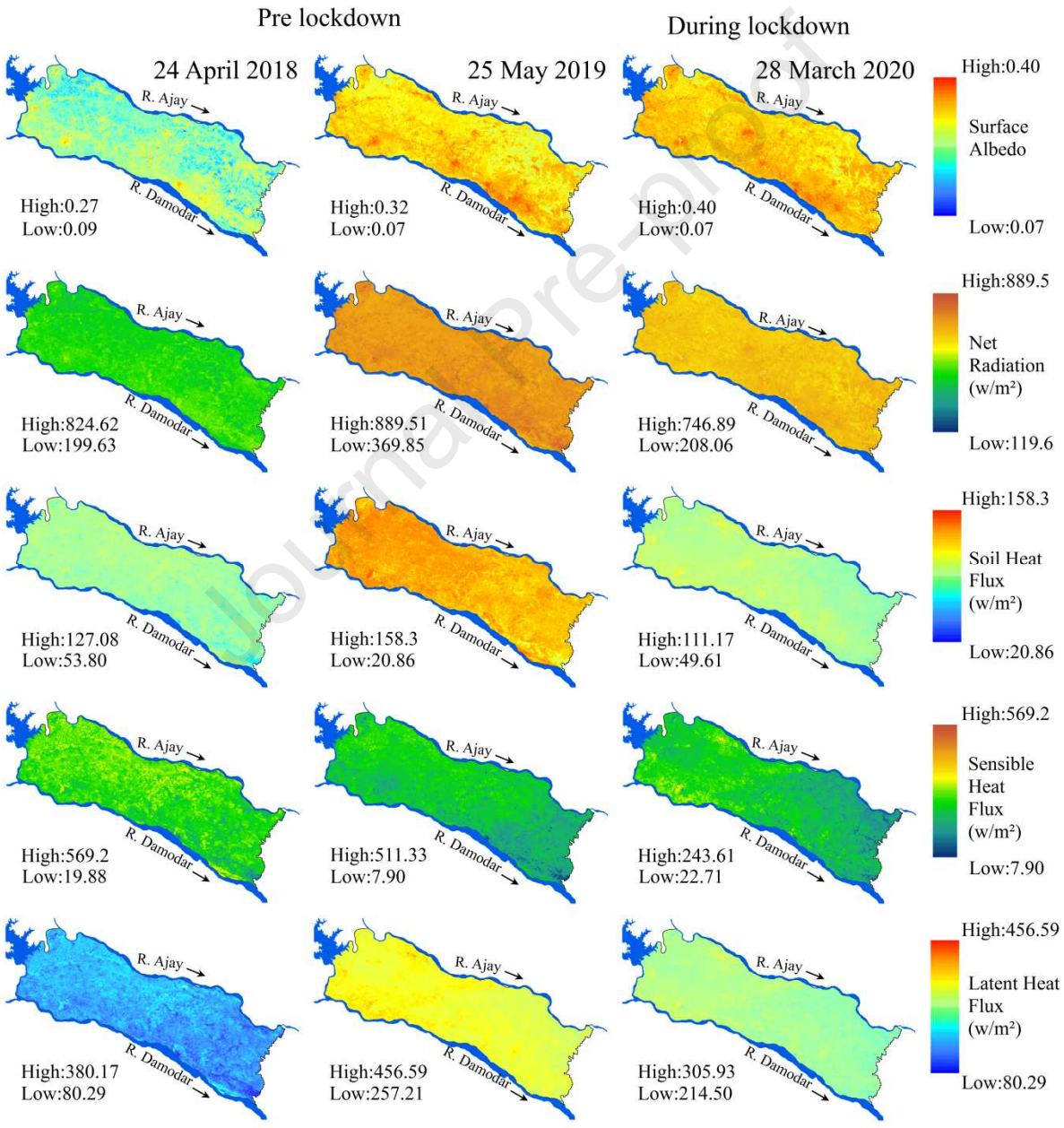

Fig. 2 Atmospheric parameters used for computing AHF

Source-specific AHF

Major sources of AHF include human metabolism (Q_M), industry (Q_I), vehicles (Q_V), and buildings (Q_B). Total anthropogenic heat emission (QF) is the sum of heat from all the mentioned sources expressed (Sailor and Lu, 2004). For computing source-specific AHF, day time metabolism rate of men, energy consumption rate in residential and commercial units, vehicle movement of different kinds were taken into account (Supplementary material 1). AHF from different sources were computed for 2018 (pre lockdown) but during lockdown extensive field survey was quite difficult. Still based on the information collected from the residents living over there regarding vehicle movement, operational state of the industries, electricity consumption state of eastern region of India (Source: Power System Operation and Cooperation or POSOCO) it was tried to estimate the possible change in AHF.

2.4 Method for showing change on air quality components

For integrating seven air quality parameters, National Air Quality Index (NAQI) of CPCB (2014) was used. For these seven air quality components (PM_{10}, $PM_{2.5}$, NO_2, NH_3, SO_2, CO, and O_3) were aggregated based on the weighted additive method. Before doing this, sub-indices for all the individual components had to be done. A detailed method for developing sub-indices and aggregation is given in Supplementary material 1. After computing all the sub-indices, the aggregated index was calculated summing up all those sub-indices.

The AQI can be interpreted about the six AQI states and their possible health threats, as mentioned by CBCB (Table 1). The health exposures consist of minimal impact which is denoted as good AQI state, where the concentration all the pollutants lies at the lowest category. Breathing discomfort starts when AQI crosses satisfactory state and reaches to moderately pollution level. In severe AQI state all pollutants reach to the worst concentration level with health impact of respiratory illness and prolonged exposure.

Table 1 Range of air quality components in National AQI classes and health impacts

	Health Impact	PM_{10} 24 hrs ($\mu g/m^3$)	$PM_{2.5}$ 24 hrs ($\mu g/m^3$)	SO_2 24 hrs ($\mu g/m^3$)	NO_2 24hrs ($\mu g/m^3$)	O_3 8hrs ($\mu g/m^3$)	CO 8 hrs (mg/m^3)	NH_3 24 hrs ($\mu g/m^3$)
		Concentration Range						
Good (0–50)	Minimal Impact	0–50	0–30	0–40	0–40	0–50	0–1	0–200
Satisfactory (51–100)	Minor breathing discomfort to sensitive people	51–100	31–60	41–80	41–80	51–100	1.1 - 2	201–400

Moderately polluted (101– 200)	Breathing discomfort to the people with lung,	101–250	61–90	81–380	81–180	101–168	2.1–10	401–800
Poor (201– 300)	Breathing discomfort to people on prolonged exposure	251–350	91–120	381–800	181–280	169–208	10–17	801–1200
Very poor (301– 400)	Respiratory illness to the people on prolonged exposure	351–430	121–250	801–1600	281–400	209–748*	17–34	1200–1800
Severe (401–500)	Respiratory illness to the people on prolonged exposure	>430	>250	>1600	>400	>748	>34	>1800

3. Results

3.1 Effect on LST, PM_{10} concentration and AHF

Figure 3 denotes spatial LST, PM_{10} and AHF states of the study area in summer seasons of 2018, 2019 and 2020 representing pre-lockdown and during lockdown periods. The range of LST was from 22ºC to 49ºC in this area with an average of 33ºC. However, immediately after implementation of lockdown in West Bengal and India, the upper limit of temperature reduced to 39ºC with much less notable change in lower limit. Average temperature reduced by >2.5 ºC within one week of lockdown. This reduction was observed over the entire study area and the rate of reduction was quite high in the industrial hubs and urban areas. For making micro level comparison, LST was classified into three classes and area under these classes was computed in pre and during lockdown periods considering study area as a whole, municipal area and municipal corporation area individually (Table 2). In the pre-lockdown period, 1584 to 1591km^2 (up to 99% of the total area) was under >30 ºC LST category, but during lockdown about 30% area from this category and shifted to relatively less intensive temperature classes. In municipal areas, the effect was almost the same in trend. In Asansol, 125 km^2 area was under >30ºC temperature class before lockdown was implemented and it squeezed to 90.51 km^2 amid lockdown implementation. In Durgapur municipal corporation area, this change was quite higher than those of the other areas. About 153 km^2 area was characterized with 30 ºC or higher surface temperature before commencing lockdown, but after commencing lockdown area under this temperature class reduced to only 37.17 km^2 (Table 2). For validating LST maps derived from image data, field driven data is taken with correlation computed. Correlation coefficient varied from 0.61 to 0.73 at 0.01 level of significance.

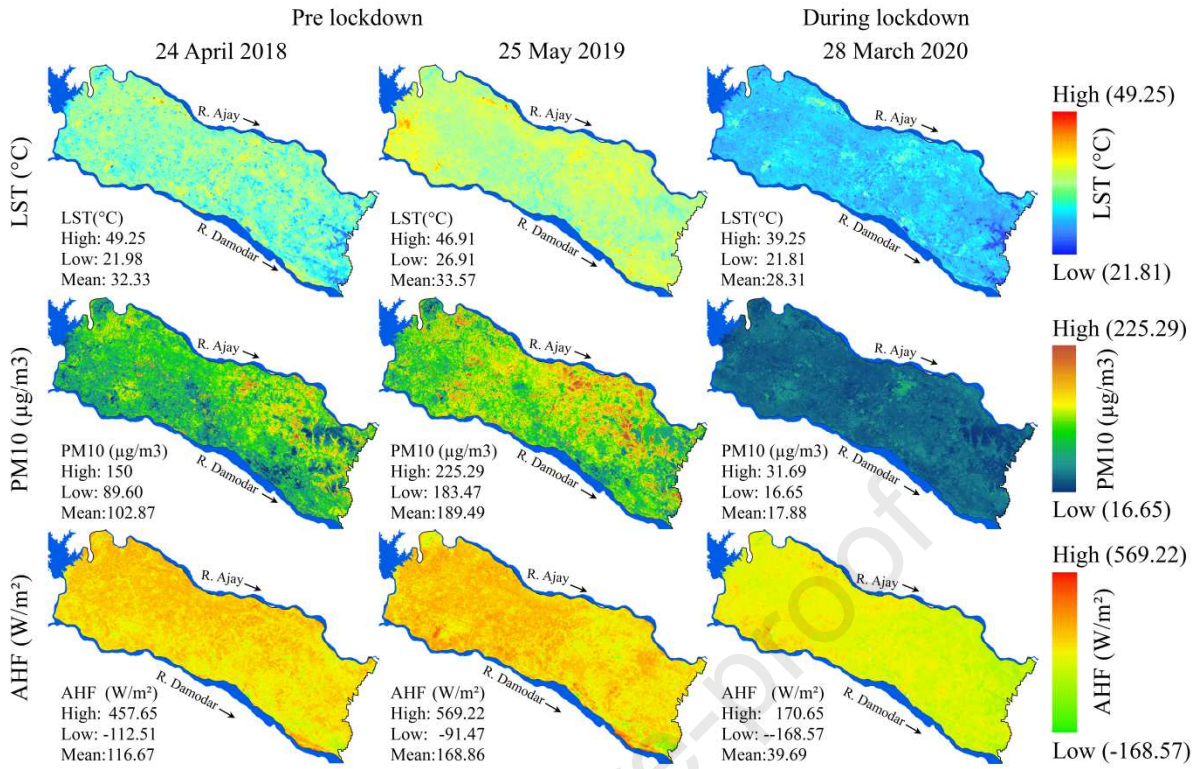

Fig. 3 LST (°C), PM_{10} (µg/m^3) and AHF (W/m^2) states computed from image data for pre and during lockdown periods

Table 2: Area (km²) under different LST classes for pre and during lockdown phases

Phase	Month	LST (°C)	ADDA Region	Asansol MC	Durgapur MC	Raniganj (M)	Jamuria (M)	Kulti (M)
Pre Lockdown	24 April (2018)	<25	1.12	0.07	0.35	0	0.10	0
		25-30	17.77	0	0.85	0	0	0.21
		>30	1584.28	124.93	153.00	24.99	79.10	95.79
	25 May (2019)	<25	0.83	0	0.00	0	0	0
		25-30	11.09	0	0.85	0	0	0.11
		>30	1591.25	125	153.35	24.99	79.20	95.89
During lockdown	28 March (2020)	<25	52.04	2.10	40.23	0.55	0.49	16.10
		25-30	600.35	32.39	76.80	14.18	14.36	29.65
		>30	950.78	90.51	37.17	10.26	64.35	50.25

Particulate matter (PM) concentration above 100µg/m^3in the atmosphere is hazardous for human health (WHO, 2016). When industries were in operational mode and urban sectors worked normally, a huge amount of PM emits to the atmosphere with average PM level exceeding the WHO defined tolerance limit. Figure 3 shows spatial distribution of PM_{10} level in pre and during lockdown periods. The range of PM_{10} level was from 89.60 to 150 µg/m^3 in

April 2018 and from 183.47 to 225.29 µg/m^3 in May 2019 (in pre lockdown period), but this range reduced to from 16.65 to 31.69 µg/m^3. Average PM_{10} levels were 102.87 and 189.49 µg/m^3 in April 2018 and May 2019, respectively, but this is only 17.88 µg/m^3 during lockdown period. This significant reduction showed that the critical level of PM_{10} concentration changed to ambient and good for human respiration. Area concentration analysis in different PM_{10} levels exhibited that in the pre-lockdown period 98.75% area was under critical PM_{10} level, but after announcing lockdown due to reduction of PM_{10} level, all parts of the study area were characterized with ambient PM level. In all the municipal areas the picture was similar (Table 3). Image derived PM_{10} data was correlated with field obtained data and correlation coefficient value was achieved between 0.43 and 0.64 at 0.01 level of significance.

Table 3 Area (km^2) under different PM_{10} classes for pre and during lockdown phases

Phase	Month	PM 10 (µg/m^3)	ADDA Region	Asansol MC	Durgapur MC	Raniganj (M)	Jamuria (M)	Kulti (M)
Pre Lockdown	24 April (2018)	<100	5.05	0	0	0	0	0
		100-125	12.16	4.8	4.03	0.28	0	0
		>125	1585.96	120.2	150.17	24.71	79.2	96
	25 May (2019)	<100	0	0	0	0	0	0
		100-125	0	0	0	0	0	0
		>125	1603.17	125.00	154.20	24.99	79.20	96.00
During lockdown	28 March (2020)	<100	1603.17	125.00	154.20	24.99	79.20	96.00
		100-125	0	0	0	0	0	0
		>125	0	0	0	0	0	0

Figure 3 shows the AHF in pre and during lockdown periods. Average AHF of 117 to 169 W/m^2 in pre-lockdown reduced to 40 W/m^2 during lockdown condition. Along with reduction of average AHF, spatial variability of AHF also significantly reduced after implementing lockdown. Area coverage under different AHF classes also shows that area under higher AHF overwhelmingly reduced during lockdown (Table 4). About 203 km^2 area was delineated AHF >100 W/m^2 in pre-lockdown period, but amid lockdown all parts of the study area were recorded with AHF <100 W/m^2. Municipal area specific analysis of the same also shows the same trend. The determinants of AHF represented in Fig. 2 shows a significant change with the implementation of lockdown. The higher limit of surface increased from 0.32 to 0.40 during lockdown whereas lower limit remained same as 0.07. Among the other factors like net radiation, soil heat flux, sensible heat flux and latent heat flux show sharp

337 decrease. Maximum limits of all three-heat flux reduced up to 50% during lockdown as
338 compared to pre lockdown situation.

339 **Table 4:** Area (km^2) under different AHF classes for pre and during lockdown phases

Year	Pre lockdown						During lockdown		
	24 April (2018)			25 May (2019)			28 March (2020)		
AHF (W/m^2) Range	<100	100-200	>200	<100	100-200	>200	<100	100-200	>200
ADPA Region	1400	193.2	9.97	1359.86	232.42	10.89	1602.65	0.52	0
Asansol MC	117.91	7.03	0.06	116.881	8.05	0.07	124.95	0.05	0
Durgapur MC	150.6	3.2	0.4	146.72	6.98	0.5	154	0.2	0
Raniganj (M)	24.01	0.97	0.01	23.75	1.23	0.01	24.99	0	0
Jamuria (M)	67.5	11.53	0.17	65.78	13.23	0.19	79.19	0.01	0
Kulti (M)	87.1	8.83	0.07	86.37	9.54	0.09	96	0	0
Mining area	10.4	7.24	0.5	10.66	6.87	0.61	18.14	0	0

340

341 Figure 4 shows the spatial pattern of source-specific AHF in the pre lockdown period.
342 Computed mean AHF from human metabolism, commercial and residential buildings,
343 industrial sector, and transport sector were 2.7, 12.96, 21.06, and 15.66 W/m^2, respectively.
344 Precisely to what extent the AHF from the mentioned sources reduced was not explored so
345 far, but supporting information can help to understand the possibility of reducing AHF. In the
346 eastern region, electricity consumption reduced by 10-20%. Maximum industries were closed
347 immediately after announcing lockdown in India. This fact explains the lowering of
348 electricity consumption. Due to the stoppage of public and private vehicles, emission from
349 transport sectors was reduced by 83%. Hence, AHF from the transport sector was likely to be
350 reduced by >80%. AHF from human metabolism will not be influenced by the lockdown
351 incident as it is the function of population density. Since 2018 to present, population density
352 has increased to some extent, and therefore, there is a possibility to increase AHF from this
353 particular source. As the proportion of AHF emission from industrial and transport sectors
354 was very high, overall, AHF possibly reduced during the lockdown as estimated from the
355 satellite image.

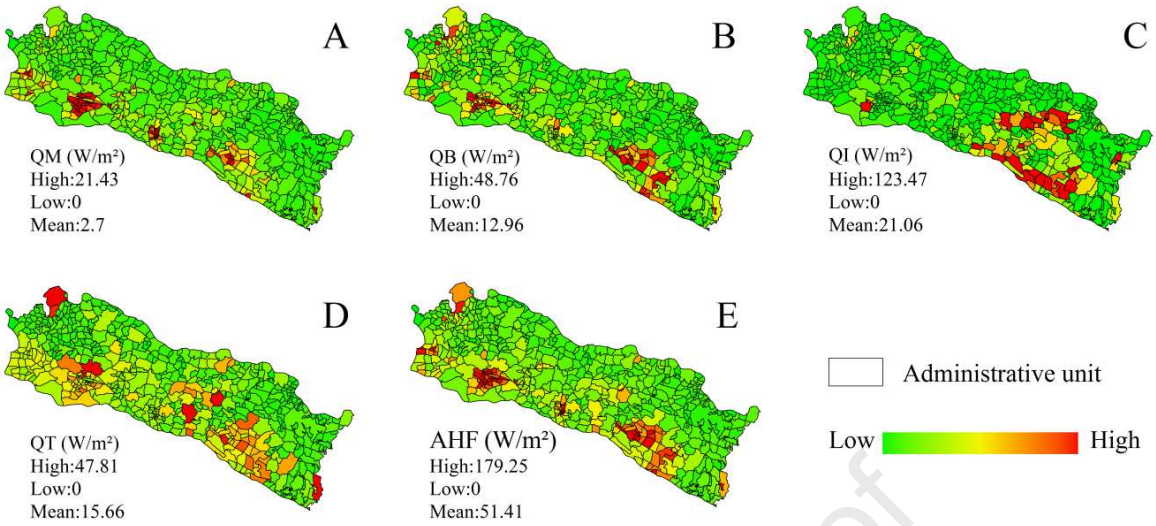

356

357 **Fig.4** Heat release from (A) Human Metabolism, (B) Commercial and Residential buildings,
358 (C) Industrial sector, (D) Transport sector and (E) Total AHF in the year of 2018

359 If it was focused on how far the LST and PM_{10} states of industrial and urban areas were
360 different from the non-industrial areas, some inference could be drawn. In the pre-lockdown
361 period, rich economic activity units including most parts of urban areas and industrial sites
362 showed positive departure of LST from mean, but in the lockdown period most parts came
363 under negative departure. More specifically, in the mining areas, 4.17% area was of negative
364 departure in the pre-lockdown period, but in the lockdown period, about 84% area registered
365 negative departure showing significant reduction of LST. When the same analysis was
366 conducted with respect to steel plants and power plant sites, an almost same trend of result
367 was identified. In this same line of thinking, when this departure analysis was carried out in
368 respect to PM 10 level, >85% areas reported negative deviation in the study region. With
369 regards to the thermal power plants, all parts of the study area were under positive PM_{10}
370 departure, but the entire region was found under negative departure from mean of all the
371 considered phases. This result shows that an industrial and urban site has responded
372 sensitively by significantly reducing the thermal intensity and pollutant level than non-urban
373 and non-industrial counterparts indicating the role of anthropogenic activities.

374 ***3.2 Effect on air quality components***

375 Figure 5 portrays the air quality components and air quality index (AQI) of the study region
376 from February to April 2020, representing both pre and during lockdown conditions. All the
377 quality components show that after implementation of lockdown pollutant level reduced to

moderate or satisfactory condition from *poor or very poor* quality. For example, $PM_{2.5}$ reduced from 98.66 to 51.3µg/m^3 signifying improvement of quality from *poor* to *satisfactory*. CP level reduced from 47 to 29 µg/m^3 showing improvement of quality from *severe to very poor* category. As the lockdown will be continued till the 3rd May 2020 or more, the quality will further be improved. In effect of the positive response of the air quality components, AQI s also improved from *poor or very poor* condition to *moderate or satisfactory* condition (Fig. 5).

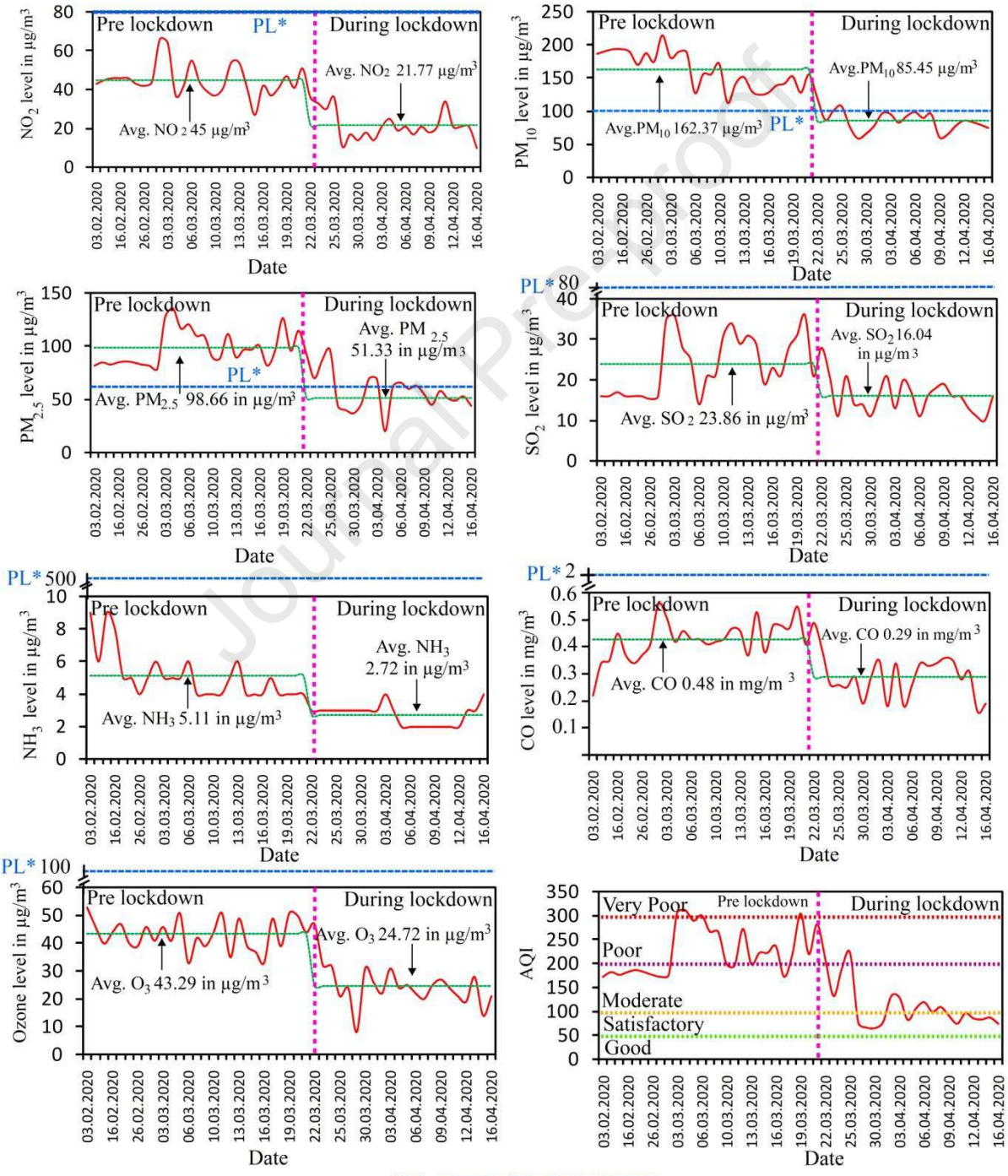

Fig. 5 Change of air quality components and AQI between pre and during lockdown periods

4. Discussion

From the results, it was very evident that lockdown has exerted a positive impact on air quality and climatic components in the highly industrialized and urbanized study area. Since implementation of complete lockdown in this region along with entire country all the major economic activities like industry, transportation, mining, public mobility, other services were completely prohibited. Almost all these activities are pollution intensive therefore, lockdown principle was able to restrict pollution generation and release. From the environmental perspective such measures were amicable to the qualitative improvement of environment in this region. The environmental compensation of lockdown was not distinctively observed in this region, as several studies carried out in different regions of world along with the satellite images of ESA and NASA categorically reported sort of similar results especially remarkable improvement of air quality (Sathe et al. 2021; Naqvi et al. 2021; Mele and Magazzino 2021; Das et al. 2021; Mor et al. 2021). In this study, it was seen that upper limit of surface temperature reduced by 20% after implementation of lockdown without having any notable change in lower limit, which signifies lowering of surface temperature in spite of having almost similar amount of solar radiation. It was witnessed in all urban-industrial centers, as the area under very hot ground surface squeezed in the municipalities. This incident clarifies the fact that industrial functioning, mining activities were the major contributors of heat source. Mixing of black aerosols ejected from the coal mining sites not only supplies a bulk amount to the concentration of particulate matter in the atmosphere, but the absorbed heat by these black particles contribute a lot to enhance atmospheric temperature. Moreover, coating of surface with these black dusts also increase the capacities of the surface to retain surface temperature, which are responsible for increasing temperature in this region. During lockdown, electricity consumption was reduced by about 20% in major industrial region. It also decelerated the fossil fuel combustion. Moreover, mining activities was almost closed in this time along with the industries. It does mean that dust admixing process was quite stopped. All these were responsible for lowering temperature condition of the study area. These processes also explain the reasons behind lowering of aerosol concentration in the atmosphere.

This study identified a decreasing trend of AHF in this area. Fossil fuel combustion is a major driver of increasing AHF (Zhang et al., 2019) which was largely stopped due the abundance

of large industrial and commercial manufacturing units. Traffic exhaust is another recognized cause behind this (Veena et al., 2020) which was noticeably restricted due to prohibition of public mobility. AHF was noticeably low in the rural areas with no signature of heavy industries. In these areas, the rate of reduction of AHF was significantly low during lockdown. It is because of non existence of heavy traffic and industry since before lockdown. Even the energy foot print of the rural India is far lower than urban and industrial counterparts.

Chen and Hu (2017) found significantly higher AHF in urban areas than the suburb areas in Beijing-Tianjin-Hebei region of northern China where they recognized vehicular traffic, industry and residential buildings as the main contributors of AHF. In present study, attenuation of heat released from two major sources namely industry and traffic largely helped to decrease the positive components of AHF like soil heat flux, sensible heat flux and latent heat flux. Temperature rise was a very well explored fact in the world due to increasing energy footprint (Aydin and Turan, 2020), but the lockdown incident adversely produced amicable results. Not only the reduction of AHF but also the disappearance of urban heat island effect was also observed in this study. The area under highest AHF category (more than 200 W/m^2) became nil in all the municipalities after commencement of lockdown. Meng et al. (2020) showed the capacity of anthropogenic heat to increase the surface temperature by simulating LST data in Beijing city and such effect can also be seen in present study area where reduction of anthropogenic heat release helped to some extent to reduce the surface temperature of industrial asphalt area. As the previous literature explored remarkable improvement of air standard during lockdown, which was also examined in this study and a promising result is observed with consideration of all parts of the study region. With the stoppage of mining sector, concentration level PM_{10} in air has started to fall with disappearance of dust emerged from the traffic greatly attributed to this fall. The same kind of result was also reported by Mandal and Pal (2020) studying stone quarrying and crushing dominated study area from Eastern India. The Sulphur containing invisible gas SO_2 released from the industries and fossil fuel driven vehicles was significantly attenuated during the progression of lockdown. As a result, overall AQI of the region shifted from very poor or poor state of pre lockdown to moderate to even satisfactory state. The reduction of power generation from power plants also attenuated the emission of NO_2 level. All these resulted in air quality improvement in pursuance of lockdown.

The rate of air quality improvement was not uniform all over the world because of the difference in land use and land cover, and different economic activity with varying intensity. This was also seen in the present study. Varying spatial PM_{10}, LST, AHF, and AQI can be explained by the existing land use and economic set up. Concentration of PM_{10} and other pollutants were usually high near the industrial units and traffic congestion area, whereas concrete ground, industrial hubs and densely populated urban settlement sites showed greater heat flux and surface temperature. In such context, another dimension of lockdown is seen in this study. The dichotomy of heat discomfort and pollution level between the area having intensive economic activity like industry, transport service and mining and the area belonging to interior countryside region reduced reasonably. It was observed in temperature as well as pollutant components. Average surface temperature of the far countryside parts of the study area was around 28˚C before lockdown started, and reduced to 27˚C amid lockdown. In intensive industry dominated and urban areas, this change was from 33˚C to 28˚C. The temperature gap between non-industrial rural areas, and urban and industrial areas was about 5˚C before lockdown, but this gap was narrowed down in lockdown (1˚C). Therefore, it clearly proves that anthropogenic activities and industrial functioning were highly responsible for higher temperature (4˚C) in the industrial and urban sectors. Consequently, it should not be conceived that 4˚C temperature was contributed from human activities. Land use transformation was another important aspect that also caused changing of thermal condition. Natural land already transformed into urban scape stimulated the thermal environment since well before lockdown. It signifies that temperature preexisting before lockdown in urban-industrial area was also partly contributed by human activities. Many studies relating to the impact of land use/land cover transformation on temperature clearly revealed that temperature in the built-up areas was 2-5˚C higher than natural ecosystem (Ziaul and Pal, 2017). Similarly, in countryside, pre-lockdown AHF was reduced from 48 to 29 W/m^2 amid lockdown and in urban-industrial area it reduced from 82 to 40 W/m^2.Here also the area specific gap was reduced by 67%. As for pollutant level, an identical trend was observed in PM_{10} concentration with concentration reduced by 75% between countryside and urban-industrial areas. These facts show the healing effect of lockdown clearly improved the environment alike the countryside region which was recognized for having healthy environment by DaSilva et al. (2017). Behind this scenario, the socio-economic parameters were found to be vital. The major economic activities of the urban-industrial areas like Asansol, Durgapur, as mentioned earlier are mainly pollution generating or heat releasing industrial production or transportation. Eventually the level of pollutants in the air and the

heat island effect remain high even in normal situation of the year. On the other hand, mainly agro or household manufacturing based economic activity and small scale transportation of the countryside release lesser pollutants or create lesser heat effect. Therefore, there was greater scope of improvement as compared to countryside. In urban-industrial area the AHF reduced to some extent due to some other socio-economic factors like complete shutdown of air-conditioned offices, hotels, malls and marts some recreational centers like auditoriums, multiplexes, restaurants etc. the commercial air-conditioned system of these places release a considerable anthropogenic heat to the surrounding. These causes were recognized by Ziaul and Pal, (2018) behind the AHF creation in another business town of eastern India. Few social festivals like several pujas (worshiping rituals), marriages, social gathering were completely prohibited amid lockdown which helped to reduces energy consumption. POSOCO data shows almost 20% reductions in average daily electricity consumption in the country during first month of lockdown implementation which was a major source of AHF release (Zhang et al., 2019).

Spatial PM_{10} concentration and AHF state were not always figured out high over all the industrial sites. Theoretically, it is not expected, but it is to be remembered that the map shows a condition of particular time. Wind may be a factor that can also plays a significant role for transporting them to the other areas. This issue was not addressed in this paper due to lack of spatial level data scarcity of wind direction and speed. If all such influencing parameters could be considered, the result would be more prominent. LST, PM_{10}, AHF and AQI simulation at different degree of urbanization, built-up density, built-up materials, green space, blue space, industrialization, emission of pollution can help us find out the threshold anthropogenic activities that could be ecologically and physiologically permissible. This could help us set a goal for pollution abatement strategies. Computation of emission level, pollution level, AHF in green technology, and efficient energy use technology used is another scope of future work that can inspire strategists and encourage a common man to rethink about the alternative option of energy use.

5. Conclusion

The present study contributed to articulate the response of a regional unit dominated by the industrial sector and densely populated urban sector in comparison to non-industrial rural parts in effects of lockdown. Moreover, most of the previous studies considered pollution parameters for showing the impact of lockdown in chiefly in urban areas, while the present

work focused on the impact of lockdown on PM_{10}, LST, and AQI along with AHF using satellite images and daily CBCB data. How far heat island effect was diluted due to stoppage of anthropogenic activities is well explained. The study explained that AHF was a noticeable contributor of urban heat and how the reduction of AHF attributed to reduced heat island effect in terms of both spatial extent and intensity. Here is the novelty of the worklies. Results exhibited reduction of LST by 4.02ºC, PM_{10} level from 102 to 18 $\mu g/m^3$, and AHF from 116 to 40 W/m^2 during lockdown period. AQI level was improved from *poor to very poor* state to *moderate to satisfactory* state. Due to lack of data source, specific AHF was not spatially estimated in lockdown condition, but change in input data for AHF computation showed the possibility of reducing AHF during lockdown. This lockdown situation is against economic production and growth of gross domestic product, and it can bring hardship among the marginal people. Therefore, lockdown is denied to be a permanent solution for checking the pollution level, while this lockdown gave a unique scope to realize how far we are responsible for changing the thermal state, pollution ambience of this region and beyond. Here is the relevance of this study. Increasing temperature in the industrial and urban environments is caused for growing thermal disconformities; increasing pollution level is caused for different predictable and unpredictable diseases. Therefore, posing control on temperature state and pollution state is highly required for our health and long life in particular and ecosystem health in general. This study clearly gives a lesson that heat and pollution emission from different anthropogenic stimulated sources is the major culprit that we must have to check for the sake of socio-economic and environmental sustainability. In this connection, prioritizing green energy, advance and efficient techniques of energy use, increase conscience and effective energy users to reduce waste are the alternatives. Optimum and economic use of energy may reduce the pollution level. To reduce heat island effect and associated human disconformities, emphasis on green space management, blue space management are some effective steps in the industrial and urban sectors. Some previous studies reported that through these steps thermal extremities could be reduced to some extent. Plantation of vegetation along road side, railways, fallow lands, roof top gardening, kitchen gardening all these are some small initiatives that could be taken for reducing heat island effect as well as pollution intensity. These steps could be partly capable to keep a balance between economic growth and environmental sustainability.

Acknowledgments:

Authors would like to thank the handling editor and anonymous reviewers for their constructive comments and suggestions to manuscript improvement.

Conflict of Interest

None

References

Ayanlade, A. and Howard, M.T., 2019. Land surface temperature and heat fluxes over three cities in Niger Delta. *Journal of African Earth Sciences*, *151*, pp.54-66. https://doi.org/10.1016/j.jafrearsci.2018.11.027

Aydin, M. and Turan, Y.E., 2020. The influence of financial openness, trade openness, and energy intensity on ecological footprint: revisiting the environmental Kuznets curve hypothesis for BRICS countries. *Environmental Science and Pollution Research*, 27(34), pp.43233-43245. https://doi.org/10.1007/s11356-020-10238-9

Bashir, M.F., Ma, B., Komal, B., Bashir, M.A., Tan, D. and Bashir, M., 2020. Correlation between climate indicators and COVID-19 pandemic in New York, USA. *Science of The Total Environment*, p.138835.https://doi.org/10.1016/j.scitotenv.2020.138835

Chakraborty, S.D., Kant, Y. and Mitra, D., 2015. Assessment of land surface temperature and heat fluxes over Delhi using remote sensing data. *Journal of Environmental Management*, *148*, pp.143-152. https://doi.org/10.1016/j.jenvman.2013.11.034

Chen, S. and Hu, D., 2017. Parameterizing anthropogenic heat flux with an energy-consumption inventory and multi-source remote sensing data. *Remote Sensing*, *9*(11), p.1165. https://doi.org/10.3390/rs9111165

Chen, Z., Hao, X., Zhang, X. and Chen, F., 2020. Have traffic restrictions improved air quality? A shock from COVID-19. *Journal of Cleaner Production*, *279*, p.123622. https://doi.org/10.1016/j.jclepro.2020.123622

Choudhury, D., Das, K. and Das, A., 2019. Assessment of land use land cover changes and its impact on variations of land surface temperature in Asansol-Durgapur Development Region. *The Egyptian Journal of Remote Sensing and Space Science*, *22*(2), pp.203-218.

CPCB (Central Pollution Control Board), 2014. Central Pollution Control Board Continuous Ambient Air Quality. http://www.cpcb.gov.in/CAAQM/frmUserAvgReportCriteria.aspx, accessed in March 2014.

Da Silva, F.B.V., do Nascimento, C.W.A., Araújo, P.R.M., da Silva, F.L. and Lima, L.H.V., 2017. Soil contamination by metals with high ecological risk in urban and rural areas. *International Journal of Environmental Science and Technology*, *14*(3), pp.553-562.

Das, P., Mandal, I., Debanshi, S., Mahato, S., Talukdar, S., Giri, B. and Pal, S., 2021. Short term unwinding lockdown effects on air pollution. *Journal of Cleaner Production*, p. 126514. https://doi.org/10.1016/j.jclepro.2021.126514

Deyong, H., Shanshan, C. and Fuzhou, D., 2017. July. Estimation of the anthropogenic heat flux distribution in Beijing-Tianjin-Hebei region based on Suomi-NPP/VIIRS nighttime light image. In *2017 IEEE International Geoscience and Remote Sensing Symposium (IGARSS)* (pp. 4012-4015). https://doi.org/10.1109/IGARSS.2017.8127880

Du, J., Park, K., Yu, X., Zhang, Y.J. and Ye, F., 2020. Massive pollutants released to Galveston Bay during Hurricane Harvey: Understanding their retention and pathway using Lagrangian numerical simulations. *Science of The Total Environment*, *704*, p.135364. https://doi.org/10.1016/j.scitotenv.2019.135364

Dutta, D. and Gupta, S., 2021. Rising Trend of Air Pollution and Its Decadal Consequences on Meteorology and Thermal Comfort Over Gangetic West Bengal, India. In *Spatial Modeling and Assessment of Environmental Contaminants* (pp. 689-720). Springer, Cham. https://doi.org/10.1007/978-3-030-63422-3_32

European Space Agency, 2020. COVID-19: nitrogen dioxide over China. https://www.esa.int/Applications/Observing_the_Earth/Copernicus/Sentinel-5 P/COVID 19_nitrogen_dioxide_over_China.

Ficetola, G.F. and Rubolini, D., 2020. Climate affects global patterns of COVID-19 early outbreak dynamics. *medRxiv*. https://doi.org/10.1101/2020.03.23.20040501

Firozjaei, M.K., Weng, Q., Zhao, C., Kiavarz, M., Lu, L. and Alavipanah, S.K., 2020. Surface anthropogenic heat islands in six megacities: An assessment based on a triple-source surface energy balance model. *Remote Sensing of Environment*, *242*, p.111751.https://doi.org/10.1016/j.rse.2020.111751

García-Santos, V., Cuxart, J., Martínez-Villagrasa, D., Jiménez, M.A. and Simó, G., 2018. Comparison of three methods for estimating land surface temperature from landsat 8-tirs sensor data. *Remote Sensing*, *10*(9), p.1450. https://doi.org/10.3390/rs10091450

Ghosh, S., Chatterjee, N.D. and Dinda, S., 2019. Relation between urban biophysical composition and dynamics of land surface temperature in the Kolkata metropolitan area: a GIS and statistical based analysis for sustainable planning. *Modeling Earth Systems and Environment*, *5*(1), pp.307-329. https://doi.org/10.1007/s40808-018-0535-9

Griffiths J, and Woodyatt A., 2020. 780 million people in China are living under travel restrictions due to the coronavirus outbreak. https://www.cnn.com/2020/02/16/asia/coronavirus-covid-19-death-toll-updateintl-hnk/index.html

https://doi.org/10.1016/j.scitotenv.2020.139281

Jin, K., Wang, F. and Wang, S., 2020. Assessing the spatiotemporal variation in anthropogenic heat and its impact on the surface thermal environment over global land areas. *Sustainable Cities and Society*, 63, p.102488. https://doi.org/10.1016/j.scs.2020.102488

Ju, M.J., Oh, J. and Choi, Y.H., 2021. Changes in air pollution levels after COVID-19 outbreak in Korea. *Science of The Total Environment*, 750, p.141521. https://doi.org/10.1016/j.scitotenv.2020.141521

Kato, S. and Yamaguchi, Y., 2005. Analysis of urban heat-island effect using ASTER and ETM+ Data: Separation of anthropogenic heat discharge and natural heat radiation from sensible heat flux. *Remote Sensing of Environment*, *99*(1-2), pp.44-54.

Kotthaus, S. and Grimmond, C.S.B., 2014. Energy exchange in a dense urban environment–Part I: Temporal variability of long-term observations in central London. *Urban Climate*, *10*, pp.261-280. https://doi.org/10.1016/j.uclim.2013.10.002

Landsat Project Science Office, 2002. Landsat 7 Science Data User's Handbook. Goddard Space FlightCenter, NASA, Washington, DC http://ltpwww.gsfc.nasa.gov/IAS/handbook/handbook_toc.html

Liou, Y.-A., Nguyen,K.A. and Ho, L.T., 2021. Altering urban greenspace patterns and heat stress risk in Hanoi City during Master Plan 2030 implementation. *Land Use Policy*, in press, 2021.

Mahato, S. and Ghosh, K.G., 2020. Short-term exposure to ambient air quality of the most polluted Indian cities due to lockdown amid SARS-CoV-2. *Environmental Research*, 188, p.109835.

Mahato, S. and Pal, S., 2018. Changing land surface temperature of a rural Rarh tract river basin of India. *Remote Sensing Applications: Society and Environment*, *10*, pp.209-223. https://doi.org/10.1016/j.rsase.2018.04.005

Mahato, S. and Pal, S., 2019. Influence of land surface parameters on the spatio-seasonal land surface temperature regime in rural West Bengal, India. *Advances in Space Research*, *63*(1), pp.172-189.https://doi.org/10.1016/j.asr.2018.09.014

Mahato, S., Pal, S. and Ghosh, K.G., 2020. Effect of lockdown amid COVID-19 pandemic on air quality of the megacity Delhi, India, Science of the Total Environment, https://doi.org/10.1016/j.scitotenv.2020.139086.

Mandal, I. and Pal, S., 2020. COVID-19 pandemic persuaded lockdown effects on environment over stone quarrying and crushing areas. *Science of The Total Environment*, p.139281.

Mandal, S., Madhipatla, K.K., Guttikunda, S., Kloog, I., Prabhakaran, D., Schwartz, J.D. and Team, G.H.I., 2020. Ensemble averaging based assessment of spatiotemporal variations in ambient PM2. 5 concentrations over Delhi, India, during 2010–2016. *Atmospheric Environment*, *224*, p.117309. https://doi.org/10.1016/j.atmosenv.2020.117309

Mele, M. and Magazzino, C., 2021. Pollution, economic growth, and COVID-19 deaths in India: a machine learning evidence. *Environmental Science and Pollution Research*, 28(3), pp.2669-2677. https://doi.org/10.1007/s11356-020-10689-0

Meng, C., Jiang, L., Jin, H., Ren, L. and Chen, T., 2020. Impact of Anthropogenic Heat on Surface Balance of Energy and Water in Beijing. Russian Meteorology and Hydrology, 45(6), pp.438-446. https://doi.org/10.3103/S1068373920060072

Mor, S., Kumar, S., Singh, T., Dogra, S., Pandey, V. and Ravindra, K., 2021. Impact of COVID-19 lockdown on air quality in Chandigarh, India: understanding the emission sources during controlled anthropogenic activities. *Chemosphere*, 263, p.127978. https://doi.org/10.1016/j.chemosphere.2020.127978

Muhammad, S., Long, X., Salman, M., 2020. COVID-19 pandemic and environmental pollution: a blessing in disguise? *Science of The Total Environment*, 138820 https://doi.org/10.1016/j. scitotenv.2020.138820

Naqvi, H.R., Datta, M., Mutreja, G., Siddiqui, M.A., Naqvi, D.F. and Naqvi, A.R., 2021. Improved air quality and associated mortalities in India under COVID-19 lockdown. *Environmental Pollution*, 268, p.115691. https://doi.org/10.1016/j.envpol.2020.115691

Nguyen, K.A. and Liou, Y.A., 2019a. Global mapping of eco-environmental vulnerability from human and nature disturbances. *Science of The Total Environment*, *664*, pp.995-1004. https://doi.org/10.1016/j.scitotenv.2019.01.407

Nguyen, K.A. and Liou, Y.A., 2019b. Mapping global eco-environment vulnerability due to human and nature disturbances. *MethodsX*, *6*, pp.862-875. https://doi.org/10.1016/j.mex.2019.03.023

Nguyen, T. H., Liou, Y.A., Nguyen, A. K., Sharma, R.C., Phien,T. D.,Liou, C.-L., and Cham, D. D., 2018. Assessing the effects of land-use types in surface urban heat islands for developing comfortable living in Hanoi City. *Remote Sensing*, 10(12), 1965, doi: 10.3390/rs10121965.

Ogunjobi, K.O., Daramola, M.T. and Akinsanola, A.A., 2018. Estimation of surface energy fluxes from remotely sensed data over Akure, Nigeria. *Spatial Information Research*, *26*(1), pp.77-89. https://doi.org/10.1007/s41324-017-0149-8

Oke, T.R. and Cleugh, H.A., 1987. Urban heat storage derived as energy balance residuals. *Boundary-Layer Meteorology*, *39*(3), pp.233-245.

Pal, S. and Ziaul, S.K., 2017. Detection of land use and land cover change and land surface temperature in English Bazar urban centre. *The Egyptian Journal of Remote Sensing and Space Science*, *20*(1), pp.125-145.https://doi.org/10.1016/j.ejrs.2016.11.003

Plocoste, T., Calif, R., Euphrasie-Clotilde, L. and Brute, F.N., 2020. Investigation of local correlations between particulate matter (PM10) and air temperature in the Caribbean basin using Ensemble Empirical Mode Decomposition. *Atmospheric Pollution Research*, 11(10), pp.1692-1704. https://doi.org/10.1016/j.apr.2020.06.031

Raj, S., Paul, S.K., Chakraborty, A. and Kuttippurath, J., 2020. Anthropogenic forcing exacerbating the urban heat islands in India. *Journal of Environmental Management*, *257*, p.110006.

Saadat, S., Rawtani, D. and Hussain, C.M., 2020. Environmental perspective of COVID-19. *Science of The Total Environment*, p.138870. https://doi.org/10.1016/j.scitotenv.2020.138870

Sailor, D.J. and Lu, L., 2004. A top–down methodology for developing diurnal and seasonal anthropogenic heating profiles for urban areas. *Atmospheric environment*, *38*(17), pp.2737-2748. https://doi.org/10.1016/j.atmosenv.2004.01.034

Saraswat, I., Mishra, R.K. and Kumar, A., 2017. Estimation of PM10 concentration from Landsat 8 OLI satellite imagery over Delhi, India. *Remote Sensing Applications: Society and Environment*, *8*, pp.251-257. https://doi.org/10.1016/j.rsase.2017.10.006

Sathe, Y., Gupta, P., Bawase, M., Lamsal, L., Patadia, F. and Thipse, S., 2021. Surface and satellite observations of air pollution in India during COVID-19 lockdown: Implication to air

quality. *Sustainable cities and society*, 66, p.102688. https://doi.org/10.1016/j.scs.2020.102688

Sharma, S., Zhang, M., Gao, J., Zhang, H. and Kota, S.H., 2020. Effect of restricted emissions during COVID-19 on air quality in India. *Science of The Total Environment*, *728*, p.138878. https://doi.org/10.1016/j.scitotenv.2020.138878

Shenoy, M., 2016. Industrial ecology in developing countries. In *Taking stock of industrial ecology* (pp. 229-245). Springer, Cham.

Tobías, A., Carnerero, C., Reche, C., Massagué, J., Via, M., Minguillón, M.C., Alastuey, A. and Querol, X., 2020. Changes in air quality during the lockdown in Barcelona (Spain) one month into the SARS-CoV-2 epidemic. *Science of The Total Environment*, p.138540. https://doi.org/10.1016/j.scitotenv.2020.138540

Travaglio, M., Yu, Y., Popovic, R., Selley, L., Leal, N.S. and Martins, L.M., 2021. Links between air pollution and COVID-19 in England. *Environmental Pollution*, 268, p.115859. https://doi.org/10.1016/j.envpol.2020.115859

Varquez, A.C.G., Kiyomoto, S. and Kanda, M., 2021. Global 1-km present and future hourly anthropogenic heat flux. *Scientific Data*, 8(1), pp.1-14. https://doi.org/10.6084/m9.figshare.13647935

Veena, K., Parammasivam, K.M. and Venkatesh, T.N., 2020. Urban Heat Island studies: Current status in India and a comparison with the International studies. *Journal of Earth System Science*, *129*(1), pp.1-15. https://doi.org/10.1007/s12040-020-1351-y

Wang, Q. and Su, M., 2020. A preliminary assessment of the impact of COVID-19 on environment–A case study of China. *Science of The Total Environment*, p.138915. https://doi.org/10.1016/j.scitotenv.2020.138915

Wang, S., Hu, D., Yu, C., Chen, S. and Di, Y., 2020. Mapping China's time-series anthropogenic heat flux with inventory method and multi-source remotely sensed data. *Science of The Total Environment*, 734, p.139457. https://doi.org/10.1016/j.scitotenv.2020.139457

Ward, H.C., Kotthaus, S., Järvi, L. and Grimmond, C.S.B., 2016. Surface Urban Energy and Water Balance Scheme (SUEWS): development and evaluation at two UK sites. *Urban Climate*, *18*, pp.1-32. https://doi.org/10.1016/j.uclim.2017.05.001

World Health Organization, 2016. Ambient Air Pollution: A Global Assessment of Exposure and Burden of Disease. World Health Organization (ISBN: 9789241511353)

Xie, X., Ai, H. and Deng, Z., 2020. Impacts of the scattered coal consumption on PM2. 5 pollution in China. *Journal of Cleaner Production*, 245, p.118922. https://doi.org/10.1016/j.scitotenv.2020.140963

Xu, Y. and Cui, G., 2021. Influence of spectral characteristics of the Earth's surface radiation on the greenhouse effect: Principles and mechanisms. *Atmospheric Environment*, 244, p.117908. https://doi.org/10.1016/j.atmosenv.2020.117908

Yu, C., Hu, D., Wang, S., Chen, S. and Wang, Y., 2021. Estimation of anthropogenic heat flux and its coupling analysis with urban building characteristics--A case study of typical cities in the Yangtze River Delta, China. *Science of The Total Environment*, p.145805. https://doi.org/10.1016/j.scitotenv.2021.145805

Zhang, G., Luo, Y. and Zhu, S., 2019. Estimation of the Spatio-Temporal Characteristics of Anthropogenic Heat Emission in the Qinhuai District of Nanjing Using the Inventory Survey Method. *Asia-Pacific Journal of Atmospheric Sciences*, pp.1-14. https://doi.org/10.1007/s13143-019-00142-9

Zhang, X., Tang, M., Guo, F., Wei, F., Yu, Z., Gao, K., Jin, M., Wang, J. and Chen, K., 2021. Associations between air pollution and COVID-19 epidemic during quarantine period in China. *Environmental Pollution*, 268, p.115897. https://doi.org/10.1016/j.envpol.2020.115897

Zhang, Y., Balzter, H. and Wu, X., 2013. Spatial–temporal patterns of urban anthropogenic heat discharge in Fuzhou, China, observed from sensible heat flux using Landsat TM/ETM+ data. *International Journal of Remote Sensing*, *34*(4), pp.1459-1477. https://doi.org/10.1080/01431161.2012.718465

Zhang, Z., Zeng, Y., Zheng, N., Luo, L., Xiao, H. and Xiao, H., 2020. Fossil fuel-related emissions were the major source of NH_3 pollution in urban cities of northern China in the autumn of 2017. *Environmental Pollution*, 256, p.113428.https://doi.org/10.1016/j.envpol.2019.113428

Zheng, Y., Huang, L. and Zhai, J., 2021. Divergent trends of urban thermal environmental characteristics in China. *Journal of Cleaner Production*, 287, p.125053. https://doi.org/10.1016/j.jclepro.2020.125053

Zhou, Y., Weng, Q., Gurney, K.R., Shuai, Y. and Hu, X., 2012. Estimation of the relationship between remotely sensed anthropogenic heat discharge and building energy use. *ISPRS Journal of Photogrammetry and Remote Sensing*, *67*, pp.65-72. https://doi.org/10.1016/j.isprsjprs.2011.10.007

Effects of lockdown due to COVID 19 outbreak on air quality and anthropogenic heat in an Industrial belt of India

Highlights

•Imposition of lockdown has reduced land surface temperature by 5 ºC
• Concentration of particulate matter 10 is decreased from 102 to 18 μg/m^3
• Anthropogenic heat flux is reduced from 116 to 40 W/m^2
• Air quality standard has improved from poor to satisfactory conditions

16 July 2020

Statement of Conflict of Interest

The authors declare that there is no conflict of interest for the manuscript entitled "**Effects of lockdown due to COVID-19 outbreak on air quality and anthropogenic heat in an industrial belt of India**" by Pal et al. submitted to the journal *Journal of Cleaner Production* for consideration of publication.

With Regards

Swades Pal, Priyanka Das, Rajesh Sarda, Indrajit Mandal, Susanta Mahato, Kim-Anh Nguyen, Yuei-An Liou, Swapan Talukdar, Tamal Kanti Saha, Sandipta Debanshi